Space 2003
23 - 25 September 2003, Long Beach, California

AIAA 2003-6268



# Microwave-propelled sails and their control

E. Chahine, C.T. Abdallah, E. Schamiloglu
Electrical & Computer Engineering Department
MSC01 1100
1 University of New Mexico
Albuquerque, NM 87131-0001
E-mail: {elias,chaouki,edl}@eece.unm.edu
& D. Goergiev
Department of Mechanical Engineering
The University of Michigan
Ann Arbor, MI 48109-2125
E-mail: dgeorgie@umich.edu

***Abstract*— This paper presents the microwave-propelled sail, its structure, assumptions. We will present its equations of motion, then we will conduct stability analysis and we will design two controllers to make it asymptotically stable and marginally stable.**

## I. Introduction

While space has intrigued humans from the beginning of time, it wasn't until the twentieth century that man began his space conquest. Though it has been almost half a century since Sputnik orbited the earth, the aerospace technology is still in its infantry with a huge potential. This paper will discuss a new generation of spacecraft, the microwave-propelled sail. The idea builds upon solar sails[4] which have been in the literature since the 1970's. The idea of microwave-propelled sails is very similar, but instead of the sun's photons hitting the solar sail at the right angle, the microwave-propelled sail alleviates that problem since we have "control" over the power source and its direction. The microwave sail architecture comprises very large ultra-weight apertures and structures. One of its distinguishing improvements is mission capability and reduction in mission cost, plus the ability of interstellar exploration missions. Microwave-propelled sails, along with solar and other types of sails will provide low-cost propulsion, and long-range mission. In [4], McInnes gives a general view on solar sails. Stability and control of carbon fiber sails propelled using microwave radiation in 1-D has been studied in [1], [2]. This paper will cover the sail shape and assumptions needed for our analysis of the sail, along with its equations of motion, and control design structure.

In this paper, we will start in section II by the physical dimensions of the sail and listing the different assumptions used, we will then describe the coordinate frames in section III, the equations of motion will be introduced in section IV, followed by a stability analysis in section V, and a linearization approach in section VI, with the presentation of two controllers in section VII, and simulation results in section VIII.

**Notation** An arrow above the symbol designates a vector, and all vectors are assumed to be column vectors, $\otimes$ refers to the quaternion multiplication,$q^*$ refers to the quaternion complex conjugate, $L_{q^*}$ is the frame rotation matrix. For any vector $\vec{v} = [v_1, v_2, v_3]^T$, the cross product operator is defined as: $\tilde{\vec{v}} = \begin{bmatrix} 0 & -v_3 & v_2 \\ v_3 & 0 & -v_1 \\ -v_2 & v_1 & 0 \end{bmatrix}$

## II. Sail

The sail studied has an umbrella-like configuration with concave sides facing the radiation source and has a bounded motion behavior. The sail is composed of a reflector made out of a light-weight carbon fiber material, a hollow mast and payload represented by a ball. The mast is attached at the reflector center of mass (CM), and connects the payload to the reflector. The payload is not directly attached to the reflector for stability reasons. To obtain passive dynamic stability :

- The reflector must be located aft of the vehicle CM for rotational stability
- The reflector must be of a concave shape such that the concave shape faces the radiation source for translational stability.

The notion of beam-riding, i.e. the stable flight of a sail propelled by Poynting flux caused by a constant power source, places considerable demands upon a sail. Even if the beam is steady, a sail can wander off the beam if its shape becomes deformed or if it does not have enough spin to keep its angular momentum aligned with the beam direction in the face of perturbations. The microwave beam pressure keeps concave shapes in tension, so concave shapes arise naturally while beam-riding. they will resist sidewise motions if the beam moves off-center, since a net sideways force restores the sail to its position (See figure 5). Therefore, our sail will have a concave shape, depicted in the figure below,1.

### A. Assumptions

In this section, we list the assumptions needed to simplify our analysis of the microwave-propelled sail.

- The system is considered as a rigid body
- The reflector has full reflectivity. The actual carbon fiber used in our experiments has 98% reflectivity.

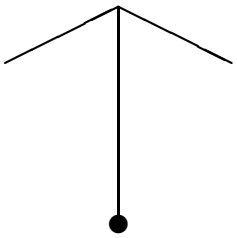

Fig. 1. Microwave sail concave shape

- There are no internal reflections.
- The payload and the mast do not block the microwave beam.
- There are no aerodynamic influences
- The microwave source is modelled as a point source with a square wave-guide.
- The gravity vector g, points towards the negative Z-axis of the inertial frame (See figure 4).

### B. Reflector model

Since we have chosen our reflector to be of a conical shape, any cross-section orthogonal to the mast is a circle. The reflector surface is created by revolving a parameterized curve about the body z-axis. The following is a fourth order polynomial approximation of the parameterized curve:

$$f(r/R) = a_0 + a_1(r/R) + a_2(r/R)^2 + a_3(r/R)^3 + a_4(r/R)^4 \quad (1)$$

where $a_0, a_1, a_2, a_3,$ and $a_4$ are shape constants, $r$ is the radial distance from the body z-axis, $R$ is the radius of the circle. We obtain a conical shape when $a_0 \neq 0$, $a_1 < 0$, and $(a_2, a_3, a_4) = 0$, with concave facing-down shape. The circle is chosen because of its symmetry and its advantages to stability. For more details on the reflector shape design, the reader is referred to [3] (See figures 2 and 3 for illustration).

## III. Coordinate Frames

There are two coordinate frames defined for this system, as depicted in figure 4: the inertial frame and the body frame. The $x_b, y_b, z_b$ axes of the body frame are attached to the vehicle CM with $z_b$ aligned with the mast axis. The inertial frame $\{X_I, Y_I, Z_I\}$ has the gravity vector in the $-Z_I$ direction. The microwave source which is represented as a point source is located on the $\{Z_I\}$ axis at $\{0, 0, -D\}$ in the inertial frame (with $D > 0$). The microwave beam radiates in the $+Z_I$ direction with its maximum intensity aligned with the $+Z_I$. The offset between the vehicle CM and the reflector CM, defined as d ($d > 0$). Since $D \gg d$ then we consider the distance from the source to the reflector CM to be D.

## IV. Equations of Motion

For a rigid body, the equations of motion are very well established,[3],[5] and [6].

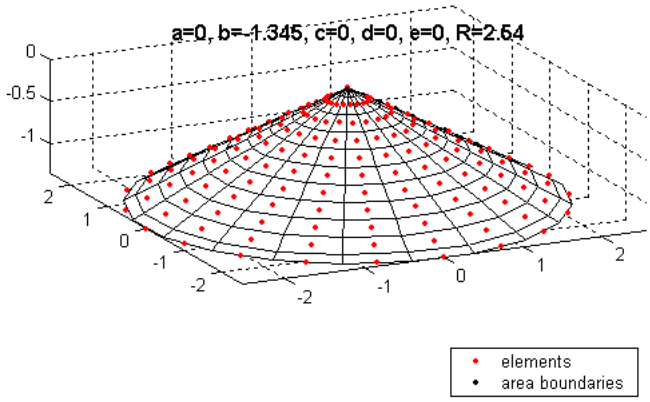


Fig. 2. Representative mesh illustrating elements and corresponding areas, notice that boundary elements require special consideration in area and normal vector calculations

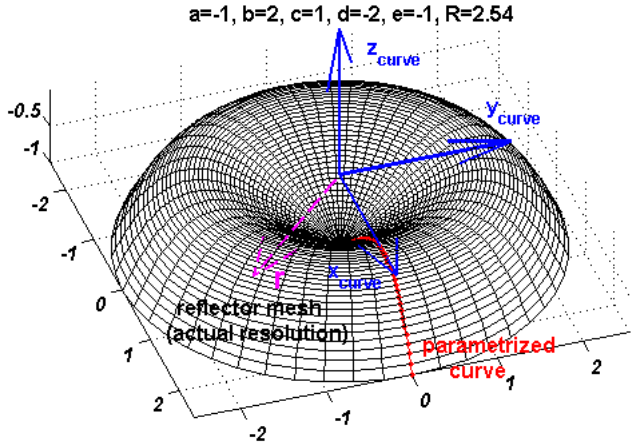


Fig. 3. Reflector mesh in MATLAB illustrating the parameterized curve

$$\dot{\vec{r}} = \vec{v} \quad (2)$$

$$\dot{\vec{v}} = \frac{\vec{F}}{m} + \vec{G} \quad (3)$$

$$\dot{\vec{q}} = \frac{1}{2}\vec{q} \otimes \vec{\omega} \quad (4)$$

$$\dot{\vec{\omega}} = J^{-1}[-\vec{\omega} \times J\vec{\omega} + \vec{T}] \quad (5)$$

$\vec{r}$ is the coordinate vector in the inertial frame $(m)$.
$\vec{v}$ as the velocity vector in the inertial frame $(m/s)$.
$\vec{q}$ is the attitude quaternion that specifies body frame orientation in inertial coordinates and $\vec{q} = [q_1; q_2; q_3; q_4] = [q_1; \vec{\alpha}]$

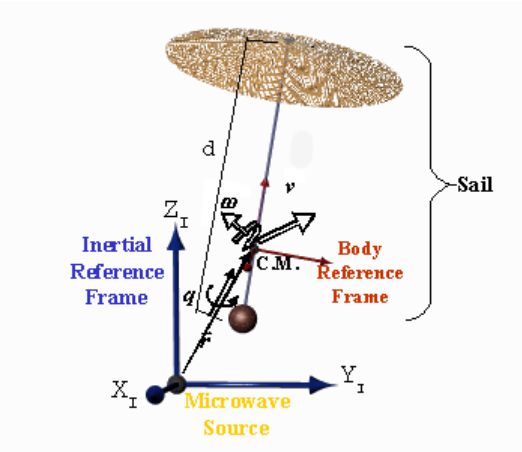


Fig. 4. Microwave sail coordinate systems and states.

$\vec{\omega}$ as the angular velocity vector in the body frame $(rad/s)$.
$m$ is the total mass of the system $(Kg)$.
$\vec{G}$ is the gravity vector such that $\vec{G} = [0, 0, -9.807]^T$ $(m/s^2)$.
J is the vehicle moment of inertia $(Kg/m^2)$.
$\vec{F}$ is the radiation-induced inertial force on the vehicle $(Kg.m/s^2)$.
$\vec{T}$ is the radiation-induced body torque on the vehicle $(Kg.m^2/s^2)$.

The force $\vec{F}$ and the torque $\vec{T}$ are given by [3]:

$$\vec{F} = \vec{q}^* \otimes \left[ 2 \int\int_{ref} dA \rho_e cos^2\psi_e \frac{\vec{\hat{n}}_{eb}}{\vec{\hat{n}}_{eb}(3)} \right] \otimes \vec{q} \tag{6}$$

$$\vec{T} = \int\int_{ref} \left( \vec{r}_{eb} \times \left[ 2 \int\int_{ref} dA \rho_e cos^2\psi_e \frac{\vec{\hat{n}}_{eb}}{\vec{\hat{n}}_{eb}(3)} \right] \right) \tag{7}$$

with $\vec{r}_{eb}$ is the vehicle CM to element location vector in the body-frame.
$\vec{\hat{n}}_{eb}$ is the reflection unit normal in the body frame at $\vec{r}_{eb}$.
$dA$ is the element area.
$\psi_e$ is the angle between the element local normal and the direction of incident radiation.
$\rho_e$ is the energy density function.

For a square wave-guide $\rho_e$ becomes

$$\rho_e = P_t \frac{(cos^2\phi cos^{n_x}\theta + sin^2\phi cos^{n_y}\theta)}{4\pi s^2} \tag{8}$$

where $P_t$ is the transmitted power.
$n_x, n_y$ are the power indices in the inertial X and Y directions respectively.
$\theta$ is the angle with the inertial Z-axis.
$\phi$ is the angle with the inertial X-axis.
$s$ is the distance from the source $\|\vec{r}\| = \sqrt{x^2 + y^2 + z^2}$

The physical control inputs to the system are therefore, $P_t, n_x$, and $n_y$. In section VII, we will design controllers using the force $\vec{F}$ and torque $\vec{T}$ and $P_t, n_x$, and $n_y$ respectively as our control inputs.

## V. Stability Analysis

Let $\vec{x} = \{\vec{r}, \vec{v}, \vec{q}, \vec{w}\}$ be the state of the system. The equations of motion are then described by the nonlinear differential equation

$$\dot{\vec{x}} = f(\vec{x}) \tag{9}$$

The equilibria for the nonlinear system $f(\vec{x}) = 0$ are obtained as $\vec{x}_0 = \{(0, 0, z_{eq}), (1, 0, 0, 0), (0, 0, 0), (0, 0, 0)\}$. Since we do not have any source of natural damping, the system can be marginally or neutrally stable at best. Basically, equilibrium is achieved when the body-frame axes are aligned (parallel) with the inertial frames axes, and the origin of the body-frame is on the inertial Z-axis, at a desired distance from the source.

Perturbations occur in translational directions represented with cylindrical coordinates, $R_I$ and $Z_I$, and in angular directions represented with the Euler angles, yaw, pitch, and roll. For most of the translational displacements, the reflector's concave shape will compensate and will bring the vehicle to equilibrium as discussed previously. The angular perturbations are more serious. When the reflector shape provides a "restoring force" effect, we notice that the force is greater on the reflector surface closest to the microwave beam leading to rotation away from equilibrium. This will cause the system to become unstable to pitch and roll perturbations. To compensate this effect, a stabilizing torque is induced by the addition of the payload. In the next section, we will attempt to get a more analytical understanding of stability through linearization.

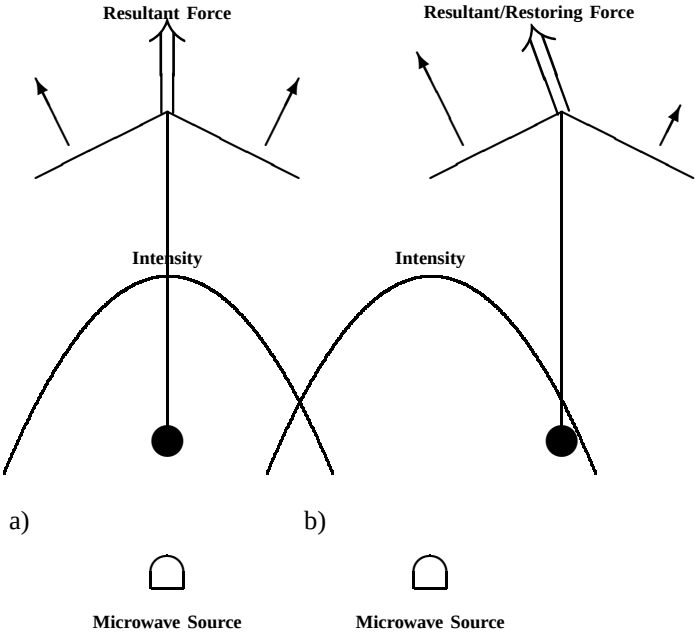


Fig. 5. A means of obtaining a 'restoring force' via reflector shape manipulation

## VI. Linearization

Using the linearization technique as a way to analyse the stability of the nonlinear system, the linearized state equation becomes:

$$\dot{\vec{x}} = A\vec{x} \tag{10}$$

where $A$ is the Jacobian evaluated at $\vec{x}_0$, $A = \frac{\partial f}{\partial \vec{x}}\Big|_{\vec{x}=\vec{x}_0}$. The stability characteristics of the linearized equations of motion are determined by the real parts of the eigenvalues of $A$. If these real parts are negative then the system is stable, unstable if they are positive, and marginally stable if the real part is zero,[7]. We mentioned in section V that the system lacks natural damping, therefore the best performance that we hope to obtain is marginal stability. The vehicle has six degrees of freedom. One is a zero frequency mode which rotates the vehicle around the $z_b$ axis. The other five are oscillatory modes. The first oscillatory mode is the bouncing or hopping mode that makes the vehicle translate up and down along the $Z_I$-axis. It is always neutrally stable. The other four are combinations of attitude and translation motion in the $Y_I Z_I$ and $X_I Z_I$ planes. They are a combination of pendulum and yo-yo modes. These four modes determine the neutral stability of the vehicle. Therefore, the system is usually unstable, and at best marginally stable,[1]. In the 1-D case, we can stabilize the microwave-propelled sail using delayed measurements,[2], and by feedback linearization,[1] . In an effort to alleviate the nonlinear constraints imposed by the system, we linearize around the origin $\vec{x}_0 = \{(0,0,z_{eq}),(1,0,0,0),(0,0,0),(0,0,0)\}$ which is considered the equilibrium point. The resulting $A$ matrix has the following eigenvalues:

$$\begin{aligned}
\lambda_{1,2} &= -137.3 \pm 144.61i \\
\lambda_{3,4} &= +137.3 \pm 144.61i \\
\lambda_{5,6} &= -46.563 \pm 1.237i \\
\lambda_{7,8} &= +46.563 \pm 1.237i \\
\lambda_{9,10} &= 0 \pm 32.258i \\
\lambda_{11} &= 0 \\
\lambda_{12} &= 0 \\
\lambda_{13} &= 0
\end{aligned}$$

We notice that the eigenvalues are conform with our analysis and the linearized system is unstable from $\lambda_{3,4}$ and $\lambda_{7,8}$ which have large positive real parts. Therefore, using the linearization technique in order to control the nonlinear system is unrealizable.

In the following sections, we will present a controller that will use nonlinear control on the force and torque, with a numerical example. Afterwards, we will investigate the statistical learning approach .

## VII. Controller

In this section, we will present two controllers. The first controller is based on the the force $\vec{F}$ and torque $\vec{T}$ and the second on $P_t, n_x$, and $n_y$.

### A. Controller I

Going back to the equations of motion and making the following changes in order to have the origin as the desired equilibrium. Let $\vec{e} = \vec{r} - \vec{r}_d$ and $\beta = q_1 - 1$. The new equations of motion become

$$\dot{\vec{e}} = \vec{v} \tag{11}$$

$$\dot{\vec{v}} = \frac{\vec{F}}{m} + \vec{G} \tag{12}$$

$$\dot{\beta} = -\frac{1}{2}\vec{\alpha}^T\vec{\omega} \tag{13}$$

$$\dot{\vec{\alpha}} = \frac{1}{2}\left(\vec{\alpha}\otimes\vec{\omega} + (\beta+1)\vec{\omega}\right) \tag{14}$$

$$\dot{\vec{\omega}} = J^{-1}[-\vec{\omega}\times J\vec{\omega} + \vec{T}] \tag{15}$$

Using the nonlinear control law given in [6] and modified in [5].

$$\vec{F} = -m\left(\vec{G} + \vec{e} + \vec{v}\right) \tag{16}$$

$$\vec{T} = -\frac{1}{2}\left[\left(\tilde{\vec{\alpha}} + (\beta+1)I\right)G_p - \gamma\beta I\right]\vec{\alpha} - G_r\vec{\omega} \tag{17}$$

where $G_p$ and $G_r$ are symmetric positive definite diagonal (3x3) matrices and $\gamma$ is a positive scalar. Let us investigate the following Lyapunov function candidate .

$$V = \frac{1}{2}\vec{e}^T\vec{e} + \frac{1}{2}\vec{v}^T\vec{v} + \gamma\beta^2 + \vec{\alpha}^T G_p\vec{\alpha} + \vec{e}^T J\vec{e} \tag{18}$$

which is defined for all $\vec{x}$ such that $\vec{x} = [\vec{e},\vec{v},\beta,\vec{\alpha},\vec{\omega}]$. The derivative of $V$ is $\dot{V} = -2\vec{\omega}^T G_r\vec{\omega} - \vec{v}^T\vec{v}$ which is negative semi-definite. Let $\Omega$ be the set where $\dot{V} = 0$. The largest invariant set in $\Omega$ is the origin.

Replacing $\vec{\omega} = 0$ and $\vec{v} = 0$ in the equations of motion, we obtain the following. $\vec{e} = 0$, $\vec{\alpha} = 0$, $\beta I = -G_p(G_p - \gamma I)^{-1}$. Since $\beta$ does not converge to zero directly, therefore we have local stability.

### B. Controller II

The actual control inputs to the system are $P_t, n_x$, and $n_y$ but they are nonlinearly related to the force and torque as seen in equations (6), (7) and (8). To avoid working with such nonlinearities, we turn to numerical methods. For simplicity purposes, we will assume that the wave-guide related parameters represented by $n_x$ and $n_y$ are constants at 3.75 each. Since the amount on the transmitted power depends mainly on the distance, we pick $P_t = P_t + \vec{K} * \vec{r}$ with $\vec{K}$ being a 3x1 gain vector. Following the examples of Vidyasagar and Koltchinskii et.al.in [8] and [9] respectively, the vector $\vec{K}$ is chosen randomly within a certain range. We chose a candidate Lyapunov function of the form $V = x'Px$ where $P$ is a diagonal matrix with positive entries within a predesigned range. The candidate Lyapunov function as chosen is always positive, but the behavior of its derivative $\dot{V} = 2\dot{x}'Px$ is unknown. The best scenario is for $\dot{V}$ to be negative.

## VIII. Numerical example

### A. Controller I

The spacecraft model used in this simulation is a scaled version of the real microwave-propelled sail. The mass is 6.11345 $g$, the inertia matrix is given by 1.0e-006 *diag([0.3368,0.3368,0.0737]) $Kg/m^2$. The initial orientation of the sail is given by the $\vec{q} = [.85; .85; .85]$ and $\beta = -0.004$. The gravitational vector is given by $G = [0; 0; -9.807]$. Using the above mentioned controller with the feedback gains chosen for $G_p = diag[100100200]$, $G_r = diag[100100100]$, and $\gamma = 100$. As you see in figure 7, $q_0$ converges almost to zero, while in figure 6, the attitude vector converges to zero at different rates to zero, depending on the values of $G_p$.

We also tested the robustness of the controller when the sail is subjected to different physical variations: shape change, area variation and random disturbance. The desired position we chose for the sail to converge to is $[x, y, z] = [1, 2, 3]$.

When we change the shape of our sail from a cone to a flat circumference and we vary the thickness of the circumference, the controller still drives the sail to the desired position, for one, five and ten levels of thickness respectively, and with all other states reaching their equilibrium.

If we "poke" holes in the surface area of the original cone-shaped sail, the controller will compensate and the sail will reach its desired location, where we have removed every second, fifth and tenth element area respectively, and with all other states converging to their equilibrium.

In case of the disturbance, we have investigated two instances.

For a random but constant disturbance whose magnitude is between 0 and 100, the maximum deviation from the desired position is 0.6115 while all other states converge to their equilibrium position. For smaller disturbances the change is barely noticeable.

For a random continuously changing force, all states go to a different equilibrium every time.

### B. Controller II

For the sake of time, we used only 48 initial conditions/plant in the vicinity of the desired equilibrium point 0 and 2 controllers in the range (0,1). We obtain the following controllers: $\vec{K_1} = [0.85800.68020.3567]$ $\vec{K_2} = [0.33580.05340.4983]$ with the diagonal matrix $P$ in the range (0,1) that yield an oscillatory behavior that is conform with marginal stability as described in [3] and shown in figures 8 and 9 . Unfortunately,the derivative of the candidate Lyapunov function was also oscillating between a negative and a positive value as seen in figure 10, therefore rendering our results purely numerical. If the range of the controller $\vec{K}$ or the diagonal matrix $P$ is increased beyond (0,1) the sail looses its marginal stability and goes unstable.

## IX. Conclusion

We have presented a general view of the microwave-propelled sail, along with its dynamics and two controllers that drive it to local stability, as was shown in our numerical examples. More work is under way for the improvement of the second controller.

## References


[1] C.T. Abdallah, E. Schamiloglu, K.A. Miller, D. Georgiev, J. Benford,and G. Benford, *Stability and control of microwave-propelled sails in 1-D*, Proceedings 2001 Space Exploration and Transportation: Journey into the Future, Albuquerque, NM, pp.552-558,February 2001.

[2] C.T. Abdallah, E. Schamiloglu, D. Georgiev, J. Benford, and G. Benford, *Control of microwave-propelled sails using delayed measurements*, Proceedings of the $19^{th}$Space Technology and applications international Forum, pp.463-468,February 2001.

[3] G. Singh, *Characterization of passive dynamic Stability of a microwave sail*, Jet Propulsion Laboratory Engineering Memorandum EM-3455-00-001, 22 March 2000.

[4] C.R. McInnes, *Solar sailing: Technology, Dynamics, and Mission Applications*, Springer-Verlag, New York, 1999.

[5] S.M.Joshi, A.G. Kelkar, J.T.-Y. Wen,G. Singh, *Robust attitude stabilization of spacecraft using nonlinear quaternion feedback*, IEEE Transactions on Automatic control, Vol. 40, Issue 10, pp. 1800-1803, October 1995.

[6] J.T. Wen and K.Kreutz-Delgado, *The attitude control problem*, IEEE Transactions on Automatic control, Vol. 36, Issue 10, October 1991.

[7] T. Kailath, *Linear systems*, Prentice Hall Information and System Sciences Series, New Jersey ,1980.

[8] V. Koltchinskii, C.T. Abdallah, M. Ariola, P. Dorato, and D. Panchenko, *Statistical learning control of uncertain systems:It is better than it seems*, UNM Technical Report: EECE,April 2000.

[9] M. Vidyasagar, *Statistical learning theory and its applications to randomized algorithms for robust controller synthesis.*, European Control Conference (ECC97), Plenary Lectures and Mini-Courses Volume, pp.162-190, Brussels, Belgium, 1997.


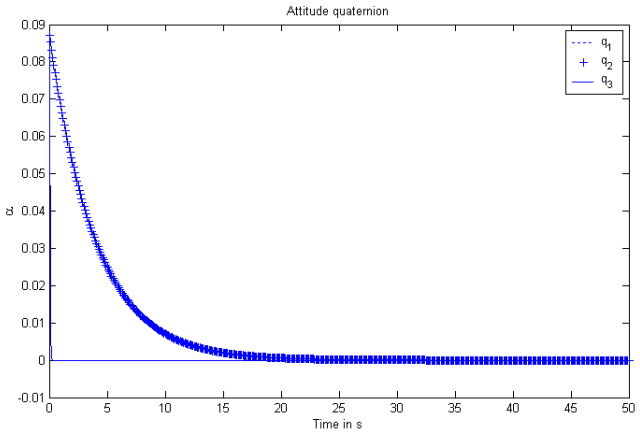


Fig. 6. Attitude vector $\vec{\alpha}$ of the sail.

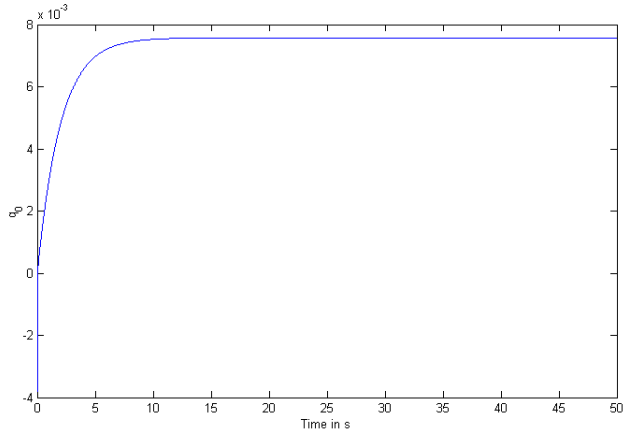


Fig. 7. $q_0$ of the attitude vector $\vec{\alpha}$.

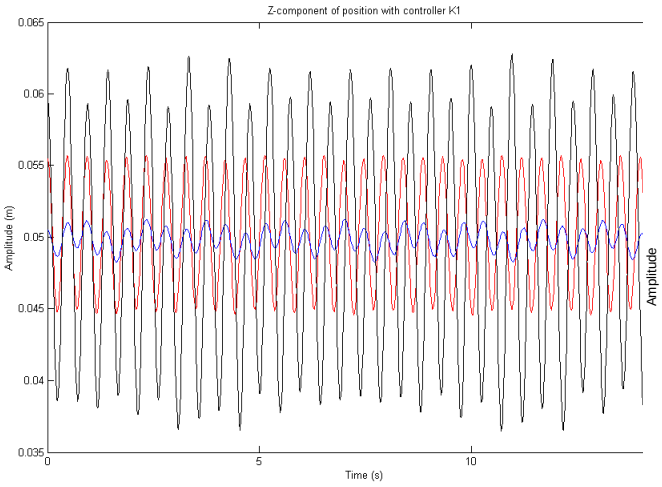


Fig. 8. Oscillatory behavior of the sail with K1

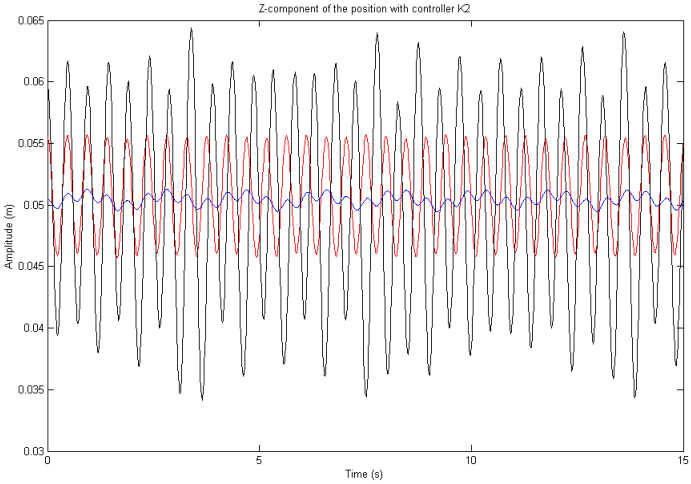


Fig. 9. Oscillatory behavior of the sail with K2

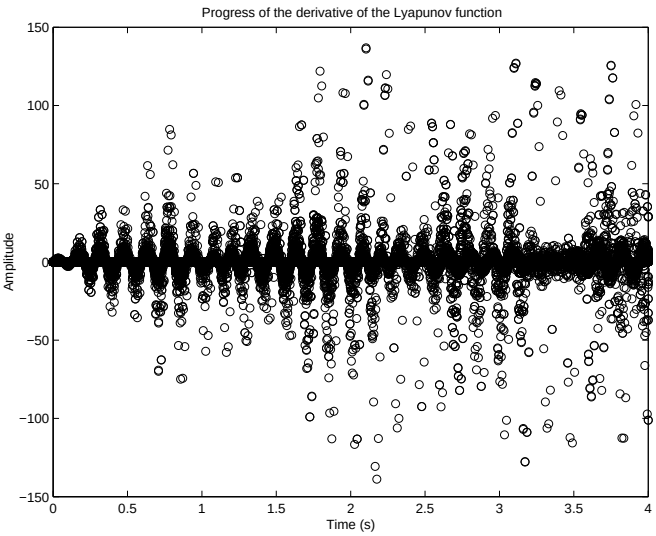


Fig. 10. The derivative of the Lyapunov function